Selected Papers

Increased Cellular Transfection with Magnetized DNA/Benzyl Amine Lipid Complexes

Mina Sakuragi, Shinichi Mochizuki, and Kazuo Sakurai*

Department of Chemistry and Biochemistry, Faculty of Engineering, The University of Kitakyushu, 1-1 Hibikino, Wakamatsu-ku, Kitakyushu, Fukuoka 808-0135

Received March 4, 2011; E-mail: sakurai@env.kitakyu-u.ac.jp

We reported that there are two possible manners in DNA localization in cationic lipid (CL)/DNA complexes and the DNA environment is strongly related to the transfection efficiency: when DNA/CL-ion complexes are in the hydrophobic phase made from the CL alkyl tails (A-type), they show low efficiency, while it is drastically increased when they are in water phase (B-type). In this paper, we prepared two types of magnetized CL/DNA complexes, denoted as MCL/DNAs from these two different DNA environments. We investigated how the external magnet field could increase the transfection efficiency comparing the two systems. We obtained higher transfection efficiency when B-type was mixed with magnetic particles. By use of electron microscopy and small-angle X-ray scattering, the structure of the MCL/DNA was determined.

Over the years, many innovative approaches have been developed for effective and safe gene delivery. Liposomes are unique model systems for studying both the structural and dynamic properties of natural membranes.[1] Liposomes can have biocompatibility, biodegradability, low toxicity, and immunogenicity, and therefore are suitable for drug delivery systems (DDS).[2] This is the main reason that many new liposome systems have been proposed for such application during the last decades. However, there have been many difficulties pointed out in extending its use in vivo. At the forefront of modern therapy, gene therapy requires genetic and cell-based technologies to treat disease, and particularly needs a good suitable DDS system. For this application, cationic lipids are generally used because they can complex with negatively charged DNA. The resultant complex is denoted as CL/DNA in this paper.

Safinya et al.[3] were the first to investigate the relationship between the supramolecular structure of CL/DNA and its transfection efficiency with synchrotron small-angle X-ray scattering (SAXS). They showed that transfection efficiency is strongly related to the structure of the CL/DNA. According to their studies, there are 2 predominant phases, a multilamellar phase where DNA monolayers are intercalated between lipid bilayers (L_α^C) and an inverted hexagonal phase where DNA is encapsulated within cationic lipid monolayered tubes and arranged on a two-dimensional hexagonal lattice (H_{II}^C). The latter structure is thought to be more suitable for transfection because inverted hexagonal structures are often observed in regions where biological membranes fuse.[4,5]

Our group reported that aromatic benzyl amine (BA), which is a cationic lipid, and amidine compounds can be used as transfection reagents because they confer better efficiency and are less toxic than commercial products.[6–9] In a previous report,[7] we examined CL/DNA consisting of DNA, BA, and 2 neutral colipids, L-α-phosphatidyl ethanolamine, dioleoyl (DOPE) and 2-dilauroyl-*sn*-glycero-3-phosphocholine (DLPC). We found the highest transfection efficiency when we used BA, DOPE, and DLPC in a ratio of 1:2:1 (B composition of B-CL). At this composition, DNA was intercalated between the preformed micellar cylinders and thus the DNA is located in the water phase. Conversely, using a 1:1 ratio of BA:DLPC (composition A), the transfection efficiency was close to 0, and we found that DNA is located in the hydrophobic layer made from the alkyl chains of CL molecules. Based on these results, we concluded that the difference in DNA localization in the CL/DNA is related to its transfection efficiency. In this study, Fe_3O_4 magnetite particles were incorporated into these two CL/DNA complexes in order to improve transfection efficiencies. We labeled the mixtures of these lipid micelles complexed with magnetite particles MCL.

Magnetic drug targeting (MDT) has become a popular approach because it can provide selective delivery to tumor targets by using an external magnetic field.[10,11] The MDT-mediated target-selectivity can minimize accumulation of drug in healthy tissues and enhances the duration of drug exposure to target. As a result, it reduces the overall amount of drug taken up by the reticuloendothelial system (RES).[12] In order to use MDT, the following parameters should be considered:[12–14] (a) the concentration and type of magnetic field, (b) the strength of the external magnetic field, and (c) the length of time the target tissue is exposed to the external magnet.

In this paper, we characterized MCLs and MCL/DNA. We also evaluated the effect of varying the MCL:DNA ratio, the concentration of magnetite particles in MCLs, and the magnetic induction time for MCL/DNA in vitro transfection efficiency by measuring luciferase activity.

Published on the web July 30, 2011; doi:10.1246/bcsj.20110071

Experimental

Materials. DOPE and DLPC were purchased from Wako chemical (Japan) and NOF corporation (Japan), respectively, and BA was synthesized using a previously reported method.[8] The solutions containing magnetite particles with a carboxylic acid group (aqueous dispersion of magnetite Fe_3O_4; mean diameter 20 nm) was purchased from Quantum Design Japan, Inc.

Preparation of MCLs and MCLs/DNA Complexes. BA, DOPE, and DLPC were dissolved in chloroform at a certain composition and freeze-dried under vacuum. The magnetic micelle solutions were prepared by adding 1 mL of fluid magnetite in 3 mM PBS at various concentrations (0.1, 0.3, and 0.5 mg mL^{-1}), and these mixtures were subsequently dispersed by ultrasonication (the lipid concentrations were 3.2 mM). The suspension was centrifuged at 1000 *g* for 15 min[15] to precipitate high density MCLs (magnetite that has reacted with BA). We retained the colloidally stable MCLs in the supernatant. MCLs with varying magnetite concentrations were denoted as 0.1-, 0.3-, and 0.5-MCLs. A micelle solution without magnetite was also prepared, denoted by CL. Plasmid DNA encoding pGL3 (bp = 5256) was amplified with *Escherichia coli* competent cells and purified by using a QIAGEN HiSpeed Plasmid Maxi kit. After estimation of the Fe_3O_4 and BA concentration by the following methods, pGL3 was added to the MCL solutions and mixed slowly after the 0.45 T magnet was placed on the side of the microtube for 5 min in order to correct the MCLs in a microtest Eppendorf tube. Then, these solutions were left at room temperature for 20 min before measurements were taken. The MCL and DNA ratio was expressed as N/P, defined by the molar ratio of nitrogen in BA to the phosphate in DNA.

Evaluation of the Incorporation Rate of the Fed Fe_3O_4 Particles. A quantitative estimate of the Fe_3O_4 particles was determined by using the chelator *o*-phenanthroline.[16,17] The MCL solution (16.7 μL) was mixed with 16.6 μL Triton X-100 solution (5%, v/v) and left for 2 days. Then we confirmed that large MCL aggregates were dissolved and transferred to small micelles by dynamic light scattering (DLS) (data not shown). Triton X-100 is a good membrane protein solubilization agent.[18] Subsequently, 83.3 μL of hydroxylamine hydrochloride solution (1.44 M) was added to the MCL and Triton X-100 mixture after ionizing the magnetite by adding 166.6 μL of 6 M HCl. After 20 min, 166.6 μL of *o*-phenanthroline solution (12.6 M) and 41.6 μL of NaOH (12 M) were added to the mixture, which was then diluted 10-fold with 50 mM citrate buffer. Finally, the magnetite concentration was estimated by reading the absorbance at 509 nm in a Jasco V-630 UV–vis spectrophotometer and determined how much Fe_3O_4 particles were incorporated into MCL comparing with the amount of the fed Fe_3O_4 particles. This value is referred to as incorporation rate of the fed Fe_3O_4 particles.

Determination of the Bound BA. The amount of BA in a given amount of MCL was determined in the following manner. MCL (40 μL) was mixed with 160 μL $CHCl_3$. The mixture was vortexed for 1 min and centrifuged for 10 min at 2000 rpm. The absorbance of the organic phase was read at 275 nm.

Small-Angle X-ray Scattering (SAXS). SAXS measurements were carried out at 40B2 SPring-8 with a 0.7 m camera using a Rigaku imaging plate (30 × 30 cm, 3000 × 3000 pixels) as a detector. The wavelength of the beam was 0.71 Å, the exposure time was 5 min, and the relative X-ray intensity and the sample transmittance were determined with 2 ion-chambers located in front of and behind the sample. We constructed a bespoke chamber for SAXS measurements that enables insertion of a sample and quartz capillary cell (2-mm diameter; Hilgenberg GmbH) and subsequent scatter measurements. One of the advantages of this vacuum set-up is to allow SAXS measurements to be taken from solutions as dilute as those used for biological assays.

Transmission Electron Microscopy (TEM). Transmission electron microscopy (TEM) was carried out for the specimens prepared using the following protocol: MCL was added to an equal volume of 2% $(NH_4)_2MoO_4$ solution and left for 1 h to negatively stain the samples. Solution was placed on a carbon-coated copper TEM grid, and the excess solution was drawn off using filter paper. After freeze-drying, TEM images were taken with a JEOL JEM 3010 at an accelerating voltage of 200 kV.

ζ-Potential and Particle Size Analyses. The ζ-potential and the mean particle sizes of MCLs and MCL/DNA were determined by DLS with a Zetasizer Nano Series (SYSMEX CORPORATION). In this instrument, the scattering angle was fixed at 173°, and the time correlation data was analyzed using the cumulant method with the attached program to obtain the size distribution profile. The ζ-potential values of samples were determined immediately following size measurements.

In Vitro Transfection Experiment. The day before the transfection experiment, 100 μL HepG2 cell suspensions in DMEM supplemented with 10% FBS and 1% penicillin–streptomycin were seeded at 1×10^5 cells/mL per well in 96 well plates. MCL/DNA with various N/P ratios and various magnetite concentrations were added to the wells (2.4 μg pDNA per well). Subsequently, a 0.5 T magnet was placed under the cell culture plate for 10, 30, and 60 min and incubated in a humidified atmosphere of 5% CO_2 at 37 °C for 2 days continuously. After transfection, the medium was replaced with DMEM supplemented with 10% FBS and incubated for further 24 h.

Cells were harvested by removing the medium, washing with 300 μL 1× PBS buffer twice, and adding 20 μL 5× lysis buffer (Promega), and then shaking for 10 min. A 10 μL aliquot of sample was mixed with 50 μL luciferin solution (Promega). The light produced over a period of 10 s was measured using a Dynatech Luminometer.

The protein content per well was determined using a Protein Quantification Kit (DOJINDO MOLECULAR TECHNOLOGIES, INC.).

Results and Discussion

Preparation and Characterization of the Ternary Complexes of Lipid/DNA/Magnetic Nanoparticles. After CL was mixed with Fe_3O_4 particles the solution was centrifuged to separate the supernatant containing MCL and CL. We presume that the major component is MCL. Figure 1 compares the Fe_3O_4 particle incorporation rate between A- and B-MCL. B-MCL showed a lower rate than A-MCL for all MCL concentrations. In terms of the number of the BA molecules binding to one particle, A-0.3MCL had 6.5×10^4, while

B-0.3MCL 5.3×10^5. The difference was about 10-fold. According to our previous work,[7] before addition of the particles, A-CL forms sphere micelles with the diameter of 4.8 nm, while B-CL forms hexagonally packed cylinders (also presented in Figure 2). The intercylinder distance is around 7 nm, which is smaller than the magnetite particle (20 nm). Therefore, in order to achieve binding, the particle has to break the hexagonal packing to enter between the cylinders. On the other hand, the sphere micelles made from A should easily form complex with the particle, because these small particles aggregate easily with the magnetite particles. These structural differences reflect the incorporation rates of the magnetite particles between them.

SAXS and TEM Images of A- and B-MCLs. Figures 2a and 2b show how the addition of the magnetite particle changed the scattering pattern for A- and B-CLs. A-MCL did not show diffraction peaks at all and showed upward deviation from the original magnetite curve that does not seem to correspond to the form factor of the micelle itself. As shown in the Supporting Information, when we changed the amount of DNA at the fixed concentrations of A-MCL, lamellar peaks appeared with increasing DNA content. This is consistent with our previous results of A-CL/DNA. This means that DNA was incorporated into the hydrophobic domain formed by A-MCL.

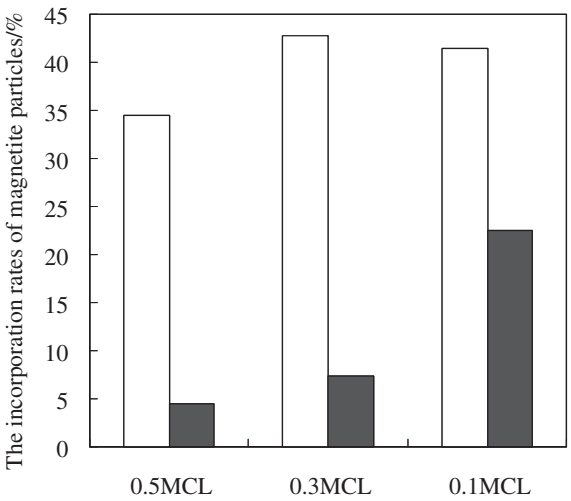

Figure 1. The incorporation rates of the magnetite particles. The white and black bars show the percentages for A- and B-MCLs, respectively.

The B-MCL SAXS showed the diffraction peaks satisfied the ratio of $1:\sqrt{3}:2$ (showed with the arrows in the figure), indicating the presence of hexagonally packed cylinders. When the magnetic particles were present, the distance between cylinders was calculated to be 6.3 nm. This value was smaller than the corresponding distance (6.9 nm) in B-CL. This difference might be due to decrease in the charge of cylinders in the solution because a part of the cationic lipid is avulsed by negatively charged magnetite due to their interaction resulting in precipitates.

Figure 3 compares the TEM images for A- and B-MCL. For A-MCL, we observed many multilamellar vesicles about 6.0 nm thick and a diameter of about 100 nm, including several magnetic particles. Since Figure 2a did not show any diffraction peak, the diffraction from the multilayer of A-MCL might be overwhelmed by intense scattering from the magnetite particles or the order of the lamellar stacking is not sufficient to give obvious diffraction. The high-q scattering in Figure 2a can be ascribed to lipid and DNA. For B-MCL, we observed some spherical objects with a diameter of about 200 nm and there were several magnetite particles included in the objects. The average size of the one object was much larger than that of A-MCL. We could observe that there were many layers running in different directions with a layer width of a few nanometer. Given the SAXS results, these layers should correspond to hexagonally packed cylinders.

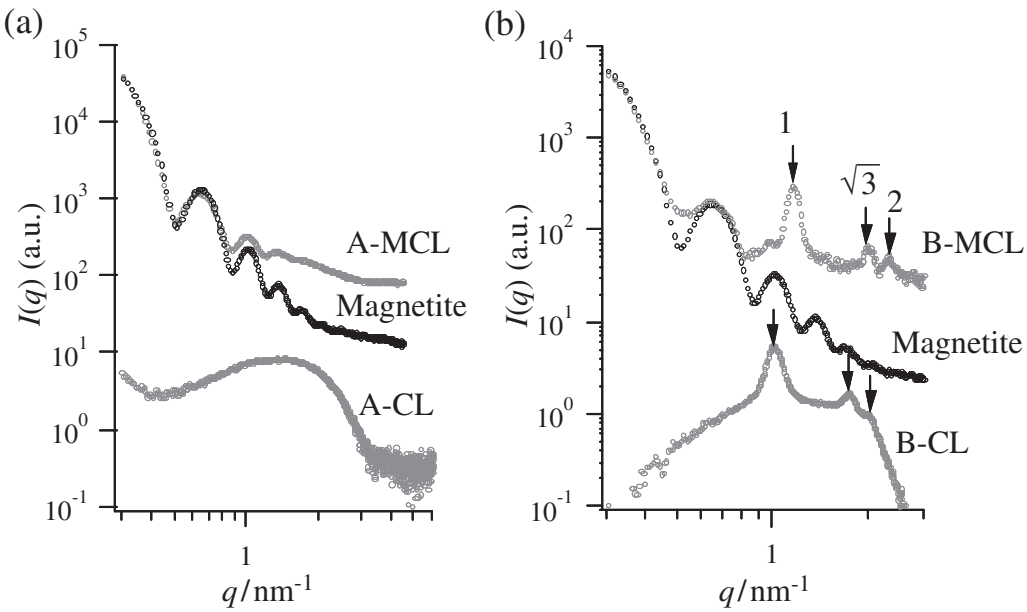

Figure 2. SAXS profiles of MCL, magnetite, and CL for composition A (a) and B (b).

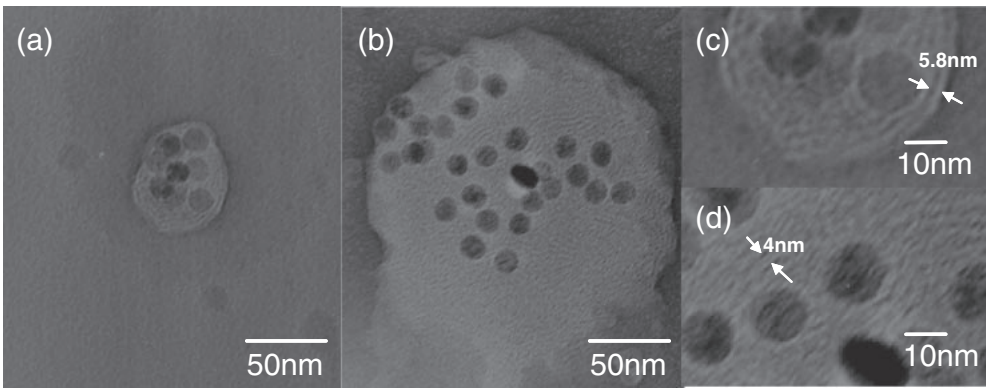

Figure 3. TEM images after staining with 1 wt % ammonium molybdate for A-MCL (a), (c), and B-MCL (b), (d). The arrows in the images (c) and (d) indicate the lipid multilayer thickness and distance between cylinders, respectively.

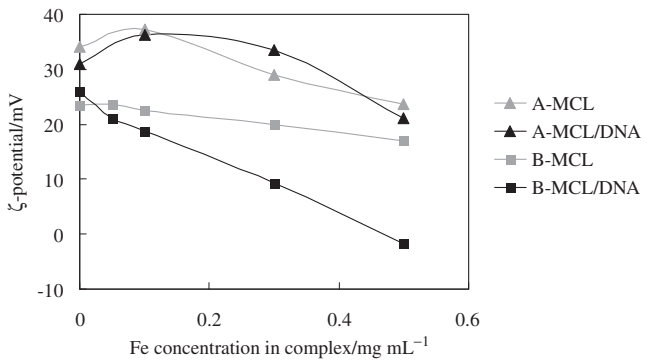

Figure 4. The mean particle ζ-potential values for MCL or MCL/DNA (N/P = 6.6).

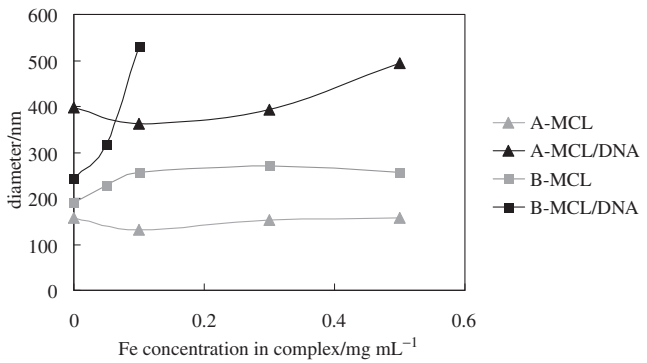

Figure 5. The mean particle size values for MCL or MCL/DNA (N/P = 6.6).

SAXS and TEM showed that several magnetite particles are encapsulated in multilamellar vesicles in A-MCL. The B-MCL TEM image, together with the fact that the magnetite particle size is 20 nm and the intercylinder distance is around 7 nm, indicates that some of the magnetite breaks apart from hexagonally packed structures and interacts with BA; most hexagonal phases, however, remain intact.

ζ-Potential and Particle Size Analyses. Figure 4 plots the ζ-potential against the Fe concentration in the complex. Since the magnetite particle is negatively charged, the ζ-potentials decreased with the addition of the magnetite particles for both A and B. These results are consistent with the ion pair formation between BA and the particles.[14,19] In the case of B, the ζ-potential for MCL/DNA decreased drastically, compared with in MCLs. On the other hand, the ζ-potential of MCL/DNA for composition A was nearly identical to that of MCLs. This result does not depend on free DNA because only the complex band was confirmed by gel electrophoresis (data not shown). We added DNA after formation of MCL and MCL itself did not show such drastic decrease of the ζ-potential. The decrease in the ζ-potential only for B-MCL/DNA can be explained by that some amount of the added DNA cannot enter between the cylinders and only attaches on the surface of the MCL aggregate.

In Figure 5, we show the approximate sizes of observed vesicles in A-MCL and spheres in B-MCL; these results are consistent with TEM results. In addition, we found that the B-MCL/DNA mean particle size was increased by increasing the magnetite concentration more than that for A-MCL/DNA. This finding is also consistent with the presence of DNA molecules on the surface of cylindrical micelles.

In Vitro Transfection Experiment. The experimental factors affecting the transfection efficiency of cationic lipids and DNA-mediated gene delivery include the cell type being transfected, N/P ratios, micelle concentration, and incubation time.[14,20] The N/P ratio is the most variable and one of the most important factors.[20] The magnetic induction time could also be an important parameter for the optimization of a magnetic target system.[14,21] In this paper, we examined the effects of N/P ratio on transfection efficiencies of A- or B-MCL/DNA at different magnetite concentrations under different magnetic inductions.

As shown in Figure 6b, B-0.3-MCL/DNA had the greatest luciferase activity at an N/P ratio of 6.6 and a magnetic induction time of 10 min for all compositions. The value is about 3.0 times greater than for MCL/DNA without external magnetic force. In the case of A-0.5-MCL/DNA, the luciferase activity was also much higher than for A-CL/DNA (Figure 6a). However, the highest value for A-MCL/DNA with an external magnetic force was about 10 times lower than that for B-MCL/DNA.

We also found that the A-MCL/DNA luciferase activity was enhanced by increasing magnetite concentration. This could be due to a weaker binding force between lipid micelles and DNA at high magnetite concentration than at low concentration because of lipids binding to magnetite particles. On the other

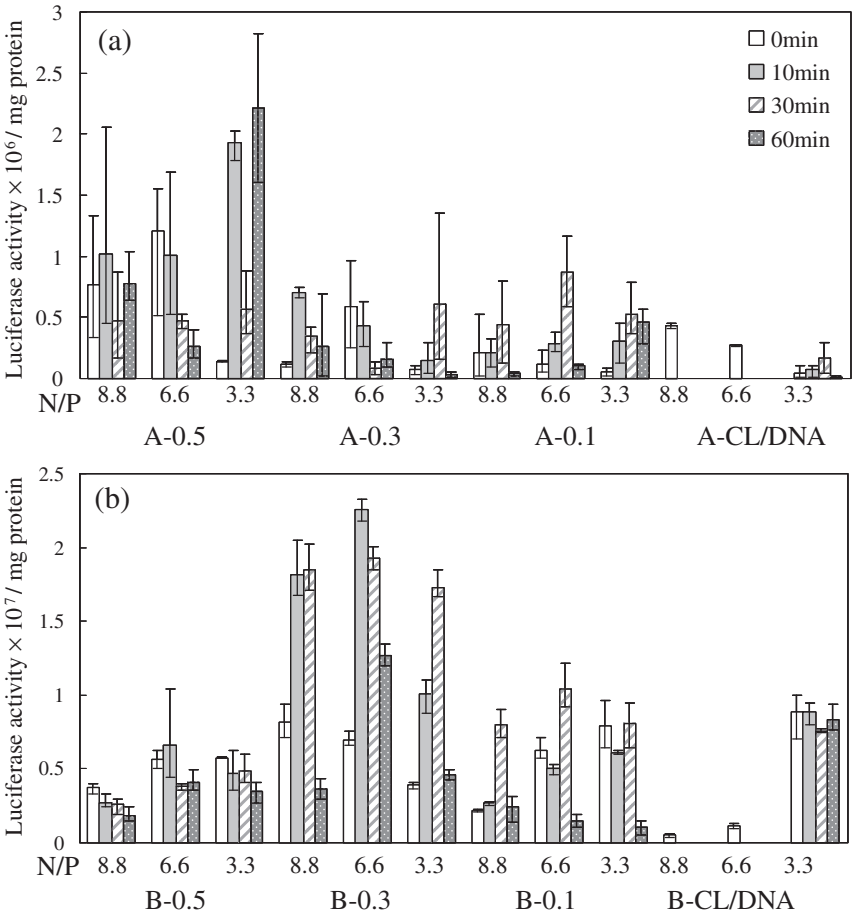

Figure 6. Effect of N/P, magnetic induction time, and Fe concentration on transfection efficiency in A-MCL/DNA (a) and B-MCL/DNA (b) in HepG2 cells. Each value represents the mean ($n = 5$).

hand, the highest activities of B-MCL/DNA were observed in B-0.3-MCL/DNA, but the activities of B-0.5-MCL/DNA with external magnetic induction were not increased compared to B-CL/DNA. This could be due to a lack of complexation between DNA molecules and 0.5-MCLs, which we observed with gel electrophoresis (data not shown). B-0.3-MCL/DNA at N/P ratio of 3.3 also did not complex with a part of the DNA molecules. Therefore, the greatest activities were observed at N/P ratio of 3.3 for both B-CL/DNA and B-0.1-MCL/DNA, while that for 0.3-MCL/DNA and 0.5-MCL/DNA was observed at N/P ratio of 6.6. This also could contribute to the aggregation state of MCL/DNA. The mean particle sizes of MCL/DNA at higher magnetite concentration or lower N/P ratio were too large to interact with cell membranes (Figure 5).

When 0.3-MCL complexed all DNA molecules (N/P = 6.6 and 8.8) without an external magnetic force, the luciferase activities were much higher than those for CL/DNA, which was presumed to be dependent on the fact that some DNA molecules in B-MCL/DNA were exposed on the surface. The surface DNA seems to interact with water-soluble proteins involved in DNA replication.

In addition, we found that longer magnetic induction for all of the compositions induced lower efficiencies. These results agreed with Zheng et al.[14] Magnetic nanoparticles could accelerate accumulation of MCL/DNA on the surface of the cells. Then intracellular nanoparticles can probably interact with cell membrane, which could result in the nonspecific changes of membrane properties such as ion transport potential and possibly fluidity or destabilization of the endosome.[14,22] These could contribute to the rapid and effective gene delivery under a magnetic field. On the other hand, longer magnetic induction could induce lower efficiencies in order to increase cellular toxicity.

Conclusion

Previously, we found that when DNA in the CL/DNA is in aqueous phase (B-type), it had high transfection efficiency, while, in the hydrophobic domain (A-type), it had low efficiency. This paper showed that the magnetization of CL/DNA by using an external magnetic force can enhance the efficiency almost 2.5 times, compared with the highest value for CL/DNA. The incorporation rate at B was much lower than that of A, which is related to the structural differences between A and B. SAXS and TEM showed that A-MCL forms multilamellar vesicles encapsulating several magnetite particles, while B-MCL forms hexagonally packed cylinders including less particles. The magnetite particles have difficulty in intercalating with cylinders of B because the size of magnetite particles is larger than the distance between the cylinders. In addition, the ζ-potential and DLS indicated the presence of DNA exposed on surface of B-MCL/DNA. Some magnetite particles in B-MCL interrupted some amount of the

added DNA intercalated between cylinders. We found that B-MCL/DNA-exposed a part of DNA molecules had higher transfection efficiency than B-CL/DNA in aqueous phase, even without an external magnetic force, but we did achieve an additional higher efficiency by using an external magnetic force. Although the A-MCL/DNA transfection efficiency was also enhanced significantly by using external magnetic force, it was much lower than that of B- MCL/DNA.

Supporting Information

Figure S1 shows the N/P dependence of SAXS profiles for compositions A and B. This material is available free of charge on the web at http://www.csj.jp/journals/bcsj/.

References

1 A. D. Bangham, *Chem. Phys. Lipids* **1993**, *64*, 275.
2 Y. Barenholz, *Curr. Opin. Colloid Interface Sci.* **2001**, *6*, 66.
3 J. O. Rädler, I. Koltover, T. Salditt, C. R. Safinya, *Science* **1997**, *275*, 810.
4 A. Lin, N. Slack, A. Ahmad, I. Koltover, C. George, C. Samuel, C. Safinta, *J. Drug Targeting* **2000**, *8*, 13.
5 *Nonviral Vectors for Gene Therapy*, ed. by L. Huang, M.-C. Hung, E. Wagner, Academic Press, **1999**.
6 K. Koiwai, K. Tokuhisa, R. Karinaga, Y. Kudo, S. Kusuki, Y. Takeda, K. Sakurai, *Bioconjugate Chem.* **2005**, *16*, 1349.
7 M. Sakuragi, S. Kusuki, E. Hamada, H. Masunaga, H. Ogawa, I. Akiba, K. Sakurai, *J. Phys.: Conf. Ser.* **2009**, *184*, 012008.
8 K. Sakurai, S. Kusuki, E. Hamada, Y. Takeda, Jpn. Kokai Tokkyo Koho 2008-143844, **2008**.
9 T. Harigai, M. Kondo, M. Isozaki, H. Kasukawa, H. Hagiwara, H. Uchiyama, J. Kimura, *Pharm. Res.* **2001**, *18*, 1284.
10 C. Alexiou, R. Jurgons, R. J. Schmid, C. Bergemann, J. Henke, W. Erhard, E. Huenges, F. Parak, *J. Drug Targeting* **2003**, *11*, 139.
11 M. Babincová, P. Babinec, V. Altanerová, Č. Altaner, P. Čičmanec, *Med. Phys.* **2004**, *31*, 2219.
12 C. Alexiou, W. Arnold, R. J. Klein, F. G. Parak, P. Hulin, C. Bergemann, W. Erhardt, S. Wagenpfeil, A. S. Lübbe, *Cancer Res.* **2000**, *60*, 6641.
13 S. Dandamudi, R. B. Campbell, *Biochim. Biophys. Acta, Biomembr.* **2007**, *1768*, 427.
14 X. Zheng, J. Lu, L. Deng, Y. Xiong, J. Chen, *Int. J. Pharm.* **2009**, *366*, 211.
15 H. Nobuto, T. Sugita, T. Kubo, S. Shimose, Y. Yasunaga, T. Murakami, M. Ochi, *Int. J. Cancer* **2004**, *109*, 627.
16 H. Kiwada, J. Sato, S. Yamada, Y. Kato, *Chem. Pharm. Bull.* **1986**, *34*, 4253.
17 R. Sabate, R. Barnadas-Rodríguez, J. Callejas-Fernández, R. Hidalgo-Álvarez, J. Estelrich, *Int. J. Pharm.* **2008**, *347*, 156.
18 O. López, A. de la Maza, L. Coderch, C. López-Iglesias, E. Wehrli, J. L. Parra, *FEBS Lett.* **1998**, *426*, 314.
19 S. Dandamudi, R. B. Campbell, *Biomaterials* **2007**, *28*, 4673.
20 N. J. Caplen, E. Kinrade, F. Sorgi, X. Gao, D. Gruenert, D. Geddes, C. Coutelle, L. Huang, E. W. Alton, R. Williamson, *Gene Ther.* **1995**, *2*, 603.
21 K. Hirao, T. Sugita, T. Kubo, K. Igarashi, K. Tanimoto, T. Murakami, Y. Yasunaga, M. Ochi, *Int. J. Oncol.* **2003**, *22*, 1065.
22 S. R. Bhattarai, S. Y. Kim, K. Y. Jang, K. C. Lee, H. K. Yi, D. Y. Lee, H. Y. Kim, P. H. Hwang, *J. Virol. Methods* **2008**, *147*, 213.